

Excited states in the large density limit: a variational approach

M P Coles¹, D E Pelinovsky¹ and P G Kevrekidis²

¹ Department of Mathematics and Statistics, McMaster University, Hamilton, Ontario, L8S 4K1 Canada

² Department of Mathematics and Statistics, University of Massachusetts, Amherst, MA 01003, USA

Received 14 October 2009, in final form 5 May 2010

Published 17 June 2010

Online at stacks.iop.org/Non/23/1753

Recommended by M J Peyrard

Abstract

Excited states of Bose–Einstein condensates are considered in the large density limit of the Gross–Pitaevskii equation with repulsive inter-atomic interactions and a harmonic potential. The relative dynamics of dark solitons (density dips on the localized condensate) with respect to the harmonic potential and to each other is approximated using the averaged Lagrangian method. This permits a complete characterization of the equilibrium positions of the dark solitons as a function of the chemical potential. It also yields an analytical handle on the oscillation frequencies of dark solitons around such equilibria. The asymptotic predictions are generalized for an arbitrary number of dark solitons and are corroborated by numerical computations for 2- and 3-soliton configurations.

Mathematics Subject Classification: 35Q55, 37K45, 37K50

(Some figures in this article are in colour only in the electronic version)

1. Introduction

The defocusing nonlinear Schrödinger equation is a prototypical model for a variety of different settings including nonlinear optics, liquids, mechanical systems and magnetic films, among others. In one spatial dimension, its prototypical excitation is the dark soliton, i.e. a localized density dip on a continuous-wave background (carrying also a phase jump).

One of the major areas of application where the description of dark solitons with a mean-field model (also known as the Gross–Pitaevskii equation) has been relevant is the physics of atomic Bose–Einstein condensates (BECs) [16, 17]. There, the repulsive inter-atomic interactions can be accurately captured by an effective nonlinear self-action [6]. A considerable volume of experimental work has conclusively demonstrated the relevance of such

nonlinear waveforms within harmonically confined condensates. Although in earlier works, such coherent structures were dynamically or thermally unstable [4, 5], more recent work has overcome such limitations [9, 18–20]. This has been achieved by working at sufficiently low temperatures (of the order of 10 nK) and for strongly confined in the transverse directions, cigar-shaped BECs. Furthermore, in these recent experiments, the nature of the generation process (e.g. by interference of two independent BECs [18, 20, 21] or through interaction of the BEC with an appropriate light pulse [19]), makes it possible to produce two or more dark solitons on the background of a localized condensate. In principle, the resulting number of dark solitons can be chosen at will, as indicated in [20].

These recent developments prompt us to examine the dynamics of dark solitons which are harmonically confined within localized repulsive BECs. These can be thought of as density dips that arise in nonlinear variants of the excited states of the quantum harmonic oscillator [3, 12]. The study of the equilibrium positions and near-equilibrium dynamics of these density dips is the principal theme of the present contribution. In particular, using a Lagrangian (variational) approach, we compute the asymptotic dependence on the chemical potential parameter both for equilibrium positions of dark solitons and for their oscillation frequencies around such equilibria.

We note that the Lagrangian approach was developed for the defocusing NLS equation without potentials in [14]. It was used for computations of stationary configurations of dark (and bright) solitary waves in single and multiple well potentials [1, 2].

This paper is organized as follows. In section 2, we present the general mathematical setup of the problem. Section 3 examines the single soliton case, section 4 extends considerations to 2-solitons and section 5 generalizes the results to an arbitrary number of m -solitons for $m \geq 2$. Section 6 compares our asymptotic predictions with numerical computations and suggests some interesting directions for further study.

2. Mathematical setup

Let us start with the Gross–Pitaevskii equation with a harmonic potential and repulsive nonlinear interactions

$$iv_\tau = -\frac{1}{2}v_{\xi\xi} + \frac{1}{2}\xi^2v + |v|^2v - \mu v, \quad (1)$$

where $v(\xi, \tau) : \mathbb{R} \times \mathbb{R} \rightarrow \mathbb{C}$ is the wave function and $\mu \in \mathbb{R}$ represents the chemical potential (and is physically associated with the number of atoms in the condensate). We are interested in localized modes of the Gross–Pitaevskii equation in the large density limit $\mu \rightarrow \infty$, which is associated with the semi-classical or Thomas–Fermi limit. Using the scaling transformation,

$$v(\xi, t) = \mu^{1/2}u(x, t), \quad \xi = (2\mu)^{1/2}x, \quad \tau = 2t, \quad (2)$$

the Gross–Pitaevskii equation (1) is transformed to the semi-classical form

$$i\varepsilon u_t + \varepsilon^2 u_{xx} + (1 - x^2 - |u|^2)u = 0, \quad (3)$$

where $u(x, t) : \mathbb{R} \times \mathbb{R} \rightarrow \mathbb{C}$ is a new wave function and $\varepsilon = (2\mu)^{-1}$ is a small parameter.

We note that the large density limit in the realm of the Gross–Pitaevskii equation (1) is of mathematical interest, yet of somewhat limited physical importance. The one-dimensional reduction of the three-dimensional condensates fails prior to the density reaching this limit. Nevertheless, all the structural features that will be observed herein will be independent of the precise form of the model and are relevant also to more elaborate non-polynomial models [20, 21] to account for the experimental observations of dark solitons in BECs.

Let η_ε be the positive solution of the stationary problem

$$\varepsilon^2 \eta_\varepsilon''(x) + (1 - x^2 - \eta_\varepsilon^2(x))\eta_\varepsilon(x) = 0, \quad x \in \mathbb{R}. \quad (4)$$

According to the previous (rigorous) results [8, 10, 11], for any sufficiently small $\varepsilon > 0$ there exists a smooth solution $\eta_\varepsilon \in C^\infty(\mathbb{R})$ that decays to zero as $|x| \rightarrow \infty$ faster than any exponential function. The ground state converges pointwise as $\varepsilon \rightarrow 0$ to the compact Thomas–Fermi cloud

$$\eta_0(x) := \lim_{\varepsilon \rightarrow 0} \eta_\varepsilon(x) = \begin{cases} (1 - x^2)^{1/2}, & \text{for } |x| \leq 1, \\ 0, & \text{for } |x| > 1. \end{cases} \quad (5)$$

Moreover, it is proved in [8] that there is $C > 0$ such that

$$\|\eta_\varepsilon - \eta_0\|_{L^\infty} \leq C\varepsilon^{1/3}. \quad (6)$$

We shall consider excited states of the Gross–Pitaevskii equation (3), which are non-positive solutions of the stationary problem

$$\varepsilon^2 u_\varepsilon''(x) + (1 - x^2 - u_\varepsilon^2(x))u_\varepsilon(x) = 0, \quad x \in \mathbb{R}. \quad (7)$$

The excited states can be classified by the number m of zeros of $u_\varepsilon(x)$ on \mathbb{R} . A unique solution with m zeros exists near $\varepsilon = \varepsilon_m$ by the local bifurcation theory [15], where $\varepsilon_m = 1/(1 + 2m)$, $m \in \mathbb{N}$. Because of the symmetry of the harmonic potential, the m th excited state $u_\varepsilon(x)$ is even on \mathbb{R} for even $m \in \mathbb{N}$ and odd on \mathbb{R} for odd $m \in \mathbb{N}$. The m th excited state is continued for $\varepsilon < \varepsilon_m$ numerically [22], based on the technique of numerical continuations from the linear states [3, 12].

In our work we shall apply variational approximations [14] to study relative dynamics of dark solitons (localized solutions with nonzero boundary conditions on the background of the positive ground state η_ε) with respect to the harmonic potential and to each other. In particular, we obtain results on the existence and spectral stability of the excited states from analysis of equilibrium positions of dark solitons and their oscillation frequencies near such equilibrium. To enable this formalism, we use the well-known product representation for vortices on the ground state [10, 11] and substitute

$$u(x, t) = \eta_\varepsilon(x)v(x, t)$$

to the Gross–Pitaevskii equation (3) and find an equivalent equation

$$i\varepsilon \eta_\varepsilon^2 v_t + \varepsilon^2 (\eta_\varepsilon^2 v_x)_x + \eta_\varepsilon^4 (1 - |v|^2)v = 0. \quad (8)$$

Excited states are solutions of the stationary equation

$$\varepsilon^2 \frac{d}{dx} (\eta_\varepsilon^2(x) V_m'(x)) + \eta_\varepsilon^4(x) (1 - V_m^2(x)) V_m(x) = 0, \quad x \in \mathbb{R}, \quad (9)$$

which have exactly m zeros on \mathbb{R} and satisfy the boundary conditions

$$\lim_{x \rightarrow \pm\infty} V_m(x) = (\pm 1)^m, \quad m \in \mathbb{N}.$$

Solutions of the stationary Gross–Pitaevskii equation (9) are critical points of the energy functional

$$\Lambda(v) = \varepsilon^2 \int_{\mathbb{R}} \eta_\varepsilon^2(x) |v_x|^2 dx + \frac{1}{2} \int_{\mathbb{R}} \eta_\varepsilon^4(x) (1 - |v|^2)^2 dx. \quad (10)$$

in the sense of $\delta\Lambda/\delta\bar{v}|_{v=V_m} = 0$. The time-dependent Gross–Pitaevskii equation (8) follows from the Lagrangian function $L(v) = K(v) + \Lambda(v)$, where

$$K(v) = \frac{i}{2} \varepsilon \int_{\mathbb{R}} \eta_\varepsilon^2(x) (v \bar{v}_t - \bar{v} v_t) dx, \quad (11)$$

by means of the Euler–Lagrange equations

$$\frac{\delta L}{\delta \bar{v}} - \frac{d}{dt} \frac{\delta L}{\delta \bar{v}_t} = 0.$$

In what follows, we obtain variational approximations for time-dependent solutions near the excited states $V_m(x)$ for $m = 1$, $m = 2$, and in the general case $m \geq 2$. We also compare these approximations with numerical results for $m = 2$ and $m = 3$.

3. 1-soliton ($m = 1$)

Let us consider the dark soliton

$$v_1(x, t) = A(t) \tanh(\varepsilon^{-1} B(t)(x - a(t))) + ib(t), \quad A > 0, \quad B > 0, \quad a \in \mathbb{R}, \quad b \in \mathbb{R}, \quad (12)$$

as an ansatz for the Lagrangian $L(v)$. The motivation for this choice originates from the fact that (12) is an exact solution of (8) if $\eta_\varepsilon = 1$ under the constraints

$$A = \sqrt{1 - b^2}, \quad B = \frac{1}{\sqrt{2}} \sqrt{1 - b^2}, \quad a = a_0 + \sqrt{2}bt, \quad b = b_0,$$

where $a_0 \in \mathbb{R}$ and $b_0 \in (-1, 1)$ are arbitrary t -independent parameters. In view of the relation

$$|v_1|^2 = A^2 + b^2 - A^2 \operatorname{sech}^2(\varepsilon^{-1} B(t)(x - a(t))),$$

it is clear that a is a centre of the dark soliton, b is its speed, A determines its amplitude and B determines its width. If the dark soliton is placed inside the confinement of the compact Thomas–Fermi cloud (5), then the constraint $a \in (-1, 1)$ has to be added.

When $\eta_\varepsilon \neq 1$, the trial function (12) is no longer an exact solution of (8) but it becomes the best approximate solution in the corresponding class of functions if parameters (A, B, a, b) are chosen from the Euler–Lagrange equations of the averaged Lagrangian $L_1(A, B, a, b) = L(v_1)$. This variational method provides a useful qualitative approximation to physicists for understanding the dynamics of dark solitons under perturbations [14]. Unlike the work of [14], we do not need to renormalize the Lagrangian function $L(v)$ thanks to the rapidly decaying weight function $\eta_\varepsilon^2(x)$ under the integration sign in (10) and (11).

Let us choose $A = \sqrt{1 - b^2}$ and $b \in (-1, 1)$ to satisfy the boundary conditions

$$\lim_{x \rightarrow \pm\infty} |v_1(x, t)| = 1 \quad \text{for all } t \in \mathbb{R}.$$

Substitution of ansatz (12) to $L(v)$ and integration in \mathbb{R} results in the effective Lagrangian

$$\begin{aligned} L(v_1) &= \frac{\varepsilon \dot{b}}{\sqrt{1 - b^2}} \int_{\mathbb{R}} \eta_\varepsilon^2(x) \tanh(z) dx + b \sqrt{1 - b^2} B \dot{a} \int_{\mathbb{R}} \eta_\varepsilon^2(x) \operatorname{sech}^2(z) dx \\ &\quad - \varepsilon b \sqrt{1 - b^2} \dot{B} B^{-1} \int_{\mathbb{R}} \eta_\varepsilon^2(x) z \operatorname{sech}^2(z) dx + (1 - b^2) B^2 \int_{\mathbb{R}} \eta_\varepsilon^2(x) \operatorname{sech}^4(z) dx \\ &\quad + \frac{1}{2} (1 - b^2)^2 \int_{\mathbb{R}} \eta_\varepsilon^4(x) \operatorname{sech}^4(z) dx, \end{aligned} \quad (13)$$

where $z = \varepsilon^{-1} B(x - a)$. Note the pointwise limits

$$\lim_{\varepsilon \rightarrow 0} \tanh(z) = \operatorname{sign}(x - a), \quad \lim_{\varepsilon \rightarrow 0} \operatorname{sech}^2(z) = 0, \quad x \in \mathbb{R} \setminus \{0\}, \quad (14)$$

which show that $\lim_{\varepsilon \rightarrow 0} L(v_1) = 0$. The asymptotic behaviour of $L(v_1)$ as $\varepsilon \rightarrow 0$ is computed in the following lemma.

Lemma 1. *Assume that $B > 0$, $a \in (-1, 1)$, and $b \in (-1, 1)$. Then,*

$$\begin{aligned} L_1 := \lim_{\varepsilon \rightarrow 0} \frac{L(v_1)}{2\varepsilon} &= -\frac{\dot{b}}{\sqrt{1 - b^2}} \left(a - \frac{1}{3} a^3 \right) + b \sqrt{1 - b^2} (1 - a^2) \dot{a} \\ &\quad + \frac{2}{3} (1 - a^2) (1 - b^2) B + \frac{1}{3B} (1 - a^2)^2 (1 - b^2)^2. \end{aligned}$$

Proof. Thanks to the limit (5), the pointwise bound (14) and the dominated convergence theorem, we have

$$\lim_{\varepsilon \rightarrow 0} \int_{\mathbb{R}} \eta_{\varepsilon}^2(x) \tanh(z) dx = \int_{-1}^1 (1 - x^2) \text{sign}(x - a) dx = -2a + \frac{2}{3}a^3,$$

To compute the remaining four integrals in (13), we use the change of variables $x \rightarrow z$, so that

$$\begin{aligned} \varepsilon^{-1} B \int_{\mathbb{R}} \eta_{\varepsilon}^2(x) \text{sech}^2(z) dx &= \int_{\mathbb{R}} \eta_{\varepsilon}^2(a + \varepsilon z B^{-1}) \text{sech}^2(z) dz \\ &= \int_{z_{-}}^{z_{+}} \eta_0^2(a + \varepsilon z B^{-1}) \text{sech}^2(z) dz + \varepsilon^{1/3} \int_{\mathbb{R}} R_{\varepsilon, B, a}(z) \text{sech}^2(z) dz, \end{aligned}$$

where $z_{\pm} = \varepsilon^{-1} B(\pm 1 - a)$ and the remainder term satisfies the uniform bound $\|R_{\varepsilon, B, a}\|_{L^{\infty}} \leq C$ for some $C > 0$, thanks to the bound (6). As a result, the second term does not contribute to the limit $\varepsilon \rightarrow 0$. To deal with the first term, we decompose the integral into three parts

$$(1 - a^2) \int_{z_{-}}^{z_{+}} \text{sech}^2(z) dz - 2\varepsilon a B^{-1} \int_{z_{-}}^{z_{+}} z \text{sech}^2(z) dz - \varepsilon^2 B^{-2} \int_{z_{-}}^{z_{+}} z^2 \text{sech}^2(z) dz.$$

We recall that the integral

$$\int_{\alpha \varepsilon^{-1}}^{\infty} z^k \text{sech}^2(z) dz, \quad k \geq 0$$

is exponentially small in ε if $\alpha > 0$ is ε -independent. As a result, the second and third terms do not contribute to the limit $\varepsilon \rightarrow 0$, while the first term gives

$$\lim_{\varepsilon \rightarrow 0} \varepsilon^{-1} B \int_{\mathbb{R}} \eta_{\varepsilon}^2(x) \text{sech}^2(z) dx = (1 - a^2) \int_{\mathbb{R}} \text{sech}^2(z) dz = 2(1 - a^2).$$

The remaining three integrals in (13) are computed similarly to the second integral in (13) and give

$$\begin{aligned} \lim_{\varepsilon \rightarrow 0} \varepsilon^{-1} B \int_{\mathbb{R}} \eta_{\varepsilon}^2(x) z \text{sech}^2(z) dx &= (1 - a^2) \int_{\mathbb{R}} z \text{sech}^2(z) dz = 0, \\ \lim_{\varepsilon \rightarrow 0} \varepsilon^{-1} B \int_{\mathbb{R}} \eta_{\varepsilon}^2(x) \text{sech}^4(z) dx &= (1 - a^2) \int_{\mathbb{R}} \text{sech}^4(z) dz = \frac{4}{3}(1 - a^2), \\ \lim_{\varepsilon \rightarrow 0} \varepsilon^{-1} B \int_{\mathbb{R}} \eta_{\varepsilon}^4(x) \text{sech}^4(z) dx &= (1 - a^2)^2 \int_{\mathbb{R}} \text{sech}^4(z) dz = \frac{4}{3}(1 - a^2)^2. \end{aligned}$$

Combining all individual computations gives the result for L_1 . ■

Since \dot{B} is absent in $L_1 := L_1(a, b, B)$, variation of L_1 with respect to B gives an algebraic equation on B with the exact solution for $a \in (-1, 1)$:

$$B = \frac{1}{\sqrt{2}} \sqrt{1 - a^2} \sqrt{1 - b^2}.$$

Eliminating B from $L_1(a, b, B)$, we simplify the effective Lagrangian to the form

$$\begin{aligned} L_1(a, b) &= \frac{2\sqrt{2}}{3} (1 - a^2)^{3/2} (1 - b^2)^{3/2} - 2\sqrt{1 - b^2} \dot{b} \left(a - \frac{1}{3}a^3 \right) \\ &\quad + \frac{d}{dt} \left[\left(a - \frac{1}{3}a^3 \right) b \sqrt{1 - b^2} \right], \end{aligned}$$

where the last term is the full derivative. Since adding a full derivative does not change the Euler–Lagrange equations, the last term can be dropped from L_1 . Variation with respect to a and b gives the following system of equations

$$\dot{a} = \sqrt{2} \sqrt{1 - a^2} b, \quad \dot{b} = -\frac{\sqrt{2} a (1 - b^2)}{\sqrt{1 - a^2}},$$

which is equivalent to the linear oscillator equation

$$\ddot{a} + 2a = 0.$$

The critical point $(a, b) = (0, 0)$ corresponds to the solution V_1 of the stationary equation (9). Oscillations near the critical point with frequency $\sqrt{2}$ correspond to the oscillations of the dark soliton V_1 relative to the positive ground state η_ε in the limit $\varepsilon \rightarrow 0$; see, e.g., [13] and references therein. This frequency was found to be the smallest nonzero frequency in the spectrum of the spectral stability problem associated with the first excited state, see figure 2 in [15].

4. 2-solitons ($m = 2$)

Let us now consider a superposition of two dark solitons

$$v_2(x, t) = [A_1(t) \tanh(\varepsilon^{-1} B_1(t)(x - a_1(t))) + ib_1(t)] \\ \times [A_2(t) \tanh(\varepsilon^{-1} B_2(t)(x - a_2(t))) + ib_2(t)], \quad (15)$$

where we shall use the relations for the individual dark solitons

$$A_j = \sqrt{1 - b_j^2}, \quad B_j = \frac{1}{\sqrt{2}} \sqrt{1 - a_j^2} \sqrt{1 - b_j^2}, \quad j = 1, 2,$$

for $a_j \in (-1, 1)$ and $b_j \in (-1, 1)$.

Although the exact solution for two dark solitons exists for the defocusing NLS equation without potentials, the variational approximations become computationally more difficult when the exact solution is used. Instead, we will use the product solution (15), which is only an approximate solution of the defocusing NLS equation if the separation distance between the dark solitons is large. Therefore, we shall later add the assumption (equation (16)) that the two dark solitons are located far away from each other compared with their widths as $\varepsilon \rightarrow 0$, although both of them are located close to the centre $x = 0$ of the harmonic potential.

In-phase oscillations of two dark solitons are very similar to the oscillations of one dark soliton and have the same frequency $\sqrt{2}$ [20] (this point is shown in section 5 for a general case of $m \geq 2$ dark solitons). Therefore, we shall consider the out-of-phase oscillations of two dark solitons and choose

$$a_1 = -a, \quad a_2 = a, \quad b_1 = -b, \quad b_2 = b,$$

with $a \in [0, 1)$ and $b \in (-1, 1)$. Substitution of v_2 to $\Lambda(v)$ gives

$$\Lambda(v_2) = A^2 B^2 \int_{\mathbb{R}} \eta_\varepsilon^2(x) [\operatorname{sech}^4(z_+) + \operatorname{sech}^4(z_-) - 2b^2 \operatorname{sech}^2(z_+) \operatorname{sech}^2(z_-) \\ - A^2 \operatorname{sech}^2(z_+) \operatorname{sech}^2(z_-) (\operatorname{sech}^2(z_+) + \operatorname{sech}^2(z_-) - 2 \tanh(z_+) \tanh(z_-))] dx \\ + \frac{1}{2} A^4 \int_{\mathbb{R}} \eta_\varepsilon^4(x) [\operatorname{sech}^4(z_+) + \operatorname{sech}^4(z_-) + 2 \operatorname{sech}^2(z_+) \operatorname{sech}^2(z_-) \\ - 2A^2 \operatorname{sech}^2(z_+) \operatorname{sech}^2(z_-) (\operatorname{sech}^2(z_+) + \operatorname{sech}^2(z_-)) + A^4 \operatorname{sech}^4(z_+) \operatorname{sech}^4(z_-)] dx,$$

where $z_\pm = \varepsilon^{-1} B(x \pm a)$. The integrals that only depend on z_+ or z_- are computed similarly to the case of 1-soliton in section 3. The overlapping integrals that depend on both z_+ and z_- are computed under the a priori assumption

$$a \leq C_1 \varepsilon^{1/6}, \quad e^{-4Ba\varepsilon^{-1}} \leq C_2 \varepsilon^2 |\log(\varepsilon)|, \quad (16)$$

for some $C_1, C_2 > 0$ and sufficiently small $\varepsilon > 0$. As we will see later, the a priori assumption allows us to recover the equilibrium state of two dark solitons and to study perturbations near the equilibrium.

After simplifications, one can write

$$\Lambda_2 := \frac{\Lambda(v_2)}{2\varepsilon} = \Lambda_+ + \Lambda_- + \Lambda_{\text{overlap}},$$

where

$$\Lambda_{\pm} := \frac{A^2 B^2}{2\varepsilon} \int_{\mathbb{R}} \eta_{\varepsilon}^2(x) \operatorname{sech}^4(z_{\pm}) dx + \frac{A^4}{4\varepsilon} \int_{\mathbb{R}} \eta_{\varepsilon}^4(x) \operatorname{sech}^4(z_{\pm}) dx$$

and

$$\begin{aligned} \Lambda_{\text{overlap}} = & -\frac{A^2 B^2}{2\varepsilon} \int_{\mathbb{R}} \eta_{\varepsilon}^2(x) \operatorname{sech}^2(z_+) \operatorname{sech}^2(z_-) \\ & \times [2b^2 + A^2 (\operatorname{sech}^2(z_+) + \operatorname{sech}^2(z_-) - 2 \tanh(z_+) \tanh(z_-))] dx \\ & + \frac{A^4}{4\varepsilon} \int_{\mathbb{R}} \eta_{\varepsilon}^4(x) \operatorname{sech}^2(z_+) \operatorname{sech}^2(z_-) \\ & \times [2 - 2A^2 (\operatorname{sech}^2(z_+) + \operatorname{sech}^2(z_-)) + A^4 \operatorname{sech}^2(z_+) \operatorname{sech}^2(z_-)] dx. \end{aligned}$$

The terms Λ_{\pm} are the potential energies of the individual dark solitons and the term Λ_{overlap} contains overlapping integrals. By lemma 1, we have

$$\Lambda_{\pm} = \frac{2\sqrt{2}}{3} (1 - a^2)^{3/2} (1 - b^2)^{3/2} + \mathcal{O}(\varepsilon^{1/3}).$$

The overlapping integrals for small ε are computed in the following lemma.

Lemma 2. Assume that $a \in (0, 1)$ satisfies (16), $b \in (-1, 1)$, and

$$A = \sqrt{1 - b^2}, \quad B = \frac{1}{\sqrt{2}} \sqrt{1 - a^2} \sqrt{1 - b^2}.$$

Then,

$$\Lambda_{\text{overlap}} = -8\sqrt{2} (1 - a^2)^{3/2} (1 - b^2)^{5/2} e^{-4Ba\varepsilon^{-1}} (1 + \mathcal{O}(\varepsilon^{1/3})).$$

Proof. To compute the overlapping integrals, we use the symmetry of the integrand and the change of variables $x \rightarrow z_-$. The first overlapping integral in Λ_{overlap} is given by

$$\begin{aligned} & \varepsilon^{-1} B \int_{\mathbb{R}} \eta_{\varepsilon}^2(x) \operatorname{sech}^2(z_+) \operatorname{sech}^2(z_-) dx \\ & = 2 \int_{-Ba\varepsilon^{-1}}^{\infty} \eta_{\varepsilon}^2(a + \varepsilon z B^{-1}) \operatorname{sech}^2(z) \operatorname{sech}^2(z + 2Ba\varepsilon^{-1}) dz, \end{aligned}$$

where $z \equiv z_-$. Similarly to the proof of lemma 1, we break the integral into four parts

$$\begin{aligned} & 2(1 - a^2) \int_{-Ba\varepsilon^{-1}}^{B(1-a)\varepsilon^{-1}} \operatorname{sech}^2(z) \operatorname{sech}^2(z + 2Ba\varepsilon^{-1}) dz \\ & - 4a\varepsilon B^{-1} \int_{-Ba\varepsilon^{-1}}^{B(1-a)\varepsilon^{-1}} z \operatorname{sech}^2(z) \operatorname{sech}^2(z + 2Ba\varepsilon^{-1}) dz \\ & - 2\varepsilon^2 B^{-2} \int_{-Ba\varepsilon^{-1}}^{B(1-a)\varepsilon^{-1}} z^2 \operatorname{sech}^2(z) \operatorname{sech}^2(z + 2Ba\varepsilon^{-1}) dz \\ & + 2\varepsilon^{1/3} \int_{-Ba\varepsilon^{-1}}^{\infty} R_{\varepsilon, B, a}(z) \operatorname{sech}^2(z) \operatorname{sech}^2(z + 2Ba\varepsilon^{-1}) dz, \end{aligned}$$

where the remainder term satisfies the bound $\|R_{\varepsilon,B,a}\|_{L^\infty} \leq C$ for some $C > 0$, thanks to the bound (6). The first part gives the leading order of the integral according to the explicit calculation

$$\begin{aligned} I_1 &= \int_{-Ba\varepsilon^{-1}}^{B(1-a)\varepsilon^{-1}} \operatorname{sech}^2(z)\operatorname{sech}^2(z+2Ba\varepsilon^{-1})dz \\ &= 16 \left(\int_{-Ba\varepsilon^{-1}}^{Ba\varepsilon^{-1}} + \int_{Ba\varepsilon^{-1}}^{B(1-a)\varepsilon^{-1}} \right) \frac{e^{-4z-4Ba\varepsilon^{-1}}}{(1+e^{-2z})^2(1+e^{-2z-4Ba\varepsilon^{-1}})^2} dz \end{aligned}$$

We have

$$0 \leq e^{-2z-4Ba\varepsilon^{-1}} \leq e^{-2Ba\varepsilon^{-1}}, \quad z \geq -Ba\varepsilon^{-1}$$

and

$$e^{-B(1-a)\varepsilon^{-1}} \ll e^{-Ba\varepsilon^{-1}}, \quad a \leq C\varepsilon^{1/6},$$

so that

$$\begin{aligned} I_1 &= 16e^{-4Ba\varepsilon^{-1}} \left(\int_{-Ba\varepsilon^{-1}}^{Ba\varepsilon^{-1}} \frac{e^{-4z}}{(1+e^{-2z})^2} dz \right) \left(1 + \mathcal{O}(e^{-2Ba\varepsilon^{-1}}) \right) + \mathcal{O}(e^{-8Ba\varepsilon^{-1}}) \\ &= 8e^{-4Ba\varepsilon^{-1}} (2Ba\varepsilon^{-1} - 1) \left(1 + \mathcal{O}(e^{-2Ba\varepsilon^{-1}}) \right). \end{aligned}$$

The second part of the overlapping integral is computed from the explicit computation

$$\begin{aligned} I_2 &= a\varepsilon \int_{-Ba\varepsilon^{-1}}^{B(1-a)\varepsilon^{-1}} z \operatorname{sech}^2(z)\operatorname{sech}^2(z+2Ba\varepsilon^{-1})dz \\ &= a\varepsilon \left(\int_{-Ba\varepsilon^{-1}}^{Ba\varepsilon^{-1}} + \int_{Ba\varepsilon^{-1}}^{B(1-a)\varepsilon^{-1}} \right) z \operatorname{sech}^2(z)\operatorname{sech}^2(z+2Ba\varepsilon^{-1})dz \\ &= \mathcal{O}(a^2 I_1) + \mathcal{O}(e^{-6Ba\varepsilon^{-1}}) = \mathcal{O}(a^2 I_1). \end{aligned}$$

The last two parts of the overlapping integrals are computed similarly and yield

$$\begin{aligned} I_3 &= \varepsilon^2 \int_{-Ba\varepsilon^{-1}}^{B(1-a)\varepsilon^{-1}} z^2 \operatorname{sech}^2(z)\operatorname{sech}^2(z+2Ba\varepsilon^{-1})dz = \mathcal{O}(a^2 I_1), \\ I_4 &= \varepsilon^{1/3} \int_{-Ba\varepsilon^{-1}}^{\infty} R_{\varepsilon,B,a}(z)\operatorname{sech}^2(z)\operatorname{sech}^2(z+2Ba\varepsilon^{-1})dz = \mathcal{O}(\varepsilon^{1/3} I_1). \end{aligned}$$

Under assumption (16), we have

$$e^{-2Ba\varepsilon^{-1}} = \mathcal{O}(\varepsilon |\log(\varepsilon)|^{1/2}) \quad \text{and} \quad a^2 = \mathcal{O}(\varepsilon^{1/3}),$$

so that we finally obtain

$$\varepsilon^{-1} B \int_{\mathbb{R}} \eta_\varepsilon^2(x) \operatorname{sech}^2(z_+) \operatorname{sech}^2(z_-) dx = 16(1 - a^2) e^{-4Ba\varepsilon^{-1}} (2Ba\varepsilon^{-1} - 1) (1 + \mathcal{O}(\varepsilon^{1/3})).$$

Similarly, we compute the other overlapping integrals in Λ_{overlap} as follows:

$$\begin{aligned} \varepsilon^{-1} B \int_{\mathbb{R}} \eta_\varepsilon^2(x) \operatorname{sech}^2(z_+) \operatorname{sech}^2(z_-) (\operatorname{sech}^2(z_+) + \operatorname{sech}^2(z_-)) dx \\ = \frac{64}{3} (1 - a^2) e^{-4Ba\varepsilon^{-1}} (1 + \mathcal{O}(\varepsilon^{1/3})), \end{aligned}$$

$$\begin{aligned} \varepsilon^{-1} B \int_{\mathbb{R}} \eta_\varepsilon^2(x) \operatorname{sech}^2(z_+) \operatorname{sech}^2(z_-) \tanh(z_+) \tanh(z_-) dx \\ = 32(1 - a^2) e^{-4Ba\varepsilon^{-1}} (-Ba\varepsilon^{-1} + 1) (1 + \mathcal{O}(\varepsilon^{1/3})) \end{aligned}$$

and

$$\varepsilon^{-1} B \int_{\mathbb{R}} \eta_{\varepsilon}^4(x) \operatorname{sech}^4(z_+) \operatorname{sech}^4(z_-) dx = 512(1 - a^2)^2 e^{-8Ba\varepsilon^{-1}} \left(Ba\varepsilon^{-1} - \frac{11}{12} \right) (1 + \mathcal{O}(\varepsilon^{1/3})).$$

Combining these computations together, we obtain the expression for Λ_{overlap} . ■

Variations of $\Lambda_2(a, b)$ define critical points that correspond to the solution $V_2(x)$ of the stationary equation (9). Since Λ_2 is even in b , the set of critical points includes the points with $b = 0$. Note that $v_2(x, t)$ in (15) is real if $b = 0$, which agrees with $V_2(x)$ being real-valued.

Since $\Lambda_+ + \Lambda_-$ is even in a and the overlapping integral is small under assumption (16), variation of $\Lambda_2(a, 0)$ in a gives a root finding problem

$$-4\sqrt{2}\varepsilon a (1 + \mathcal{O}(\varepsilon^{1/3})) + 32e^{-2\sqrt{2}a\varepsilon^{-1}} (1 + \mathcal{O}(\varepsilon^{1/3})) = 0, \quad (17)$$

where we recall that $a^2 = \mathcal{O}(\varepsilon^{1/3})$. The asymptotic analysis of the roots of the nonlinear equation (17) in the following lemma shows that the a priori assumption (16) is indeed satisfied.

Lemma 3. *For sufficiently small $\varepsilon > 0$, there exists a simple root of the nonlinear equation (17) in the neighbourhood of 0, which is expanded by*

$$a = \frac{\varepsilon}{\sqrt{2}} \left(-\log(\varepsilon) - \frac{1}{2} \log |\log(\varepsilon)| + \frac{3}{2} \log(2) + o(1) \right) \quad \text{as } \varepsilon \rightarrow 0. \quad (18)$$

Proof. Taking a natural logarithm of the nonlinear equation (17), we obtain

$$2\sqrt{2}a + \varepsilon \log(a) = -\varepsilon \log(\varepsilon) + \frac{5}{2}\varepsilon \log(2) + \mathcal{O}(\varepsilon^{4/3}).$$

Let $a = -\frac{1}{\sqrt{2}}\varepsilon \log(\varepsilon)U$ and rewrite the problem for U :

$$U - \frac{\log(U)}{2 \log(\varepsilon)} = 1 + \frac{\log |\log(\varepsilon)|}{2 \log(\varepsilon)} - \frac{3 \log(2)}{2 \log(\varepsilon)} (1 + \mathcal{O}(\varepsilon^{1/3})). \quad (19)$$

By the implicit function theorem applied to equation (19), existence of a unique root $U(\varepsilon)$ in a one-sided neighbourhood of $\varepsilon > 0$ is proved, where $U(\varepsilon)$ is continuous in $\varepsilon > 0$ and $\lim_{\varepsilon \downarrow 0} U(\varepsilon) = 1$. To estimate the remainder term for $|U(\varepsilon) - 1|$, one can further decompose

$$U = 1 + \frac{\log |\log(\varepsilon)|}{2 \log(\varepsilon)} (1 + V)$$

and rewrite the problem for V :

$$V - \frac{\log(1 + (\log |\log(\varepsilon)|/2 \log(\varepsilon))(1 + V))}{\log |\log(\varepsilon)|} = -\frac{3 \log(2)}{\log |\log(\varepsilon)|} (1 + \mathcal{O}(\varepsilon^{1/3})). \quad (20)$$

By the implicit function theorem applied again to equation (20), existence of a unique root $V(\varepsilon)$ in a one-sided neighbourhood of $\varepsilon > 0$ is proved, where $V(\varepsilon)$ is continuous in $\varepsilon > 0$ and

$$\lim_{\varepsilon \downarrow 0} \log |\log(\varepsilon)| \left(V(\varepsilon) + \frac{3 \log(2)}{\log |\log(\varepsilon)|} \right) = 0.$$

Substitution of U and V back to formula for a gives (18). ■

By lemma 3, we can study temporal dynamics of two dark solitons near the bound state that corresponds to a small root of the nonlinear equation (17).

To proceed with time-derivative terms, we substitute (15) to the kinetic part $K(v)$ in (11) and find that

$$K_2 := \frac{K(v_2)}{2\varepsilon} = K_+ + K_- + K_{\text{overlap}},$$

where

$$K_{\pm} = \mp \frac{\dot{b}}{2\sqrt{1-b^2}} \int_{\mathbb{R}} \eta_{\varepsilon}^2(x) \tanh(z_{\pm}) dx + \frac{b\sqrt{1-b^2}B\dot{a}}{2\varepsilon} \int_{\mathbb{R}} \eta_{\varepsilon}^2(x) \operatorname{sech}^2(z_{\pm}) dx$$

$$\pm \frac{b\sqrt{1-b^2}\dot{B}}{2B} \int_{\mathbb{R}} \eta_{\varepsilon}^2(x) z_{\pm} \operatorname{sech}^2(z_{\pm}) dx$$

and

$$K_{\text{overlap}} = \frac{1}{2} \dot{b}(1-b^2)^{1/2} \int_{\mathbb{R}} \eta_{\varepsilon}^2(x) (\tanh(z_+) \operatorname{sech}^2(z_-) - \tanh(z_-) \operatorname{sech}^2(z_+)) dx$$

$$- \varepsilon^{-1} b(1-b^2)^{3/2} (B\dot{a} + \dot{B}a) \int_{\mathbb{R}} \eta_{\varepsilon}^2(x) \operatorname{sech}^2(z_+) \operatorname{sech}^2(z_-) dx.$$

The terms K_{\pm} are the kinetic energies of the individual dark solitons and the term K_{overlap} contains overlapping integrals. By lemma 1, we have

$$\lim_{\varepsilon \rightarrow 0} (K_+ + K_-) = -4\sqrt{1-b^2}\dot{b} \left(a - \frac{1}{3}a^3 \right) + 2 \frac{d}{dt} \left[\left(a - \frac{1}{3}a^3 \right) b\sqrt{1-b^2} \right].$$

The overlapping integrals for small ε are estimated in the following lemma.

Lemma 4. Assume that $a \in (0, 1)$ satisfies (16), $b \in (-1, 1)$, and

$$A = \sqrt{1-b^2}, \quad B = \frac{\sqrt{1-a^2}\sqrt{1-b^2}}{\sqrt{2}}.$$

Then,

$$K_{\text{overlap}} = 2\varepsilon \dot{b}(1-b^2)^{1/2} B^{-1}(1-a^2) (1 + \mathcal{O}(\varepsilon^{1/3}))$$

$$- 16b(1-b^2)^{3/2} (\dot{a} + B^{-1}\dot{B}a)(1-a^2) e^{-4Ba\varepsilon^{-1}} (2Ba\varepsilon^{-1} - 1) (1 + \mathcal{O}(\varepsilon^{1/3})).$$

Proof. Both terms in K_{overlap} are estimated similarly to the proof of lemma 2. ■

To obtain effective dynamical equations on (a, b) valid in the domain specified by assumption (16), we expand $L_2(a, b) = L(v_2)/2\varepsilon$ in the quadratic form in (a, b) and apply the limit $\varepsilon \rightarrow 0$ to all but the overlapping integrals. As a result, the reduced effective Lagrangian $L_2(a, b)$ takes the form

$$L_2(a, b) \sim \frac{4\sqrt{2}}{3} (1 - \frac{3}{2}(b^2 + a^2) + \mathcal{O}(b^2 + a^2)^2) - 4a\dot{b} (1 + \mathcal{O}(b^2 + a^2))$$

$$- 8\sqrt{2}e^{-2\sqrt{2}a\varepsilon^{-1}(1+\mathcal{O}(b^2+a^2))} (1 + \mathcal{O}(b^2 + a^2)).$$

In variables (a, b) , the Euler–Lagrange equations at the leading order become

$$\dot{a} = \sqrt{2}b, \quad \dot{b} = -\sqrt{2}a + 8\varepsilon^{-1}e^{-2\sqrt{2}a\varepsilon^{-1}}$$

or, equivalently, recover the nonlinear oscillator equation

$$\ddot{a} + 2a = 8\sqrt{2}\varepsilon^{-1}e^{-2\sqrt{2}a/\varepsilon}.$$

The equilibrium state is given by the root $a_0(\varepsilon)$, which satisfies the asymptotic expansion (18). This equilibrium state is a centre and linear oscillations near the centre satisfy

$$\ddot{\delta} + \omega_0^2\delta = 0,$$

where $\delta = a - a_0(\varepsilon)$ and

$$\omega_0^2(\varepsilon) = 2 + \frac{32}{\varepsilon^2} e^{-2\sqrt{2}a_0(\varepsilon)\varepsilon^{-1}} = 2 + \frac{4\sqrt{2}a_0(\varepsilon)}{\varepsilon}$$

$$= -4 \log(\varepsilon) - 2 \log |\log(\varepsilon)| + 2 + 6 \log(2) + o(1), \quad \text{as } \varepsilon \rightarrow 0, \quad (21)$$

thanks to lemma 3. We note that the frequency $\omega_0(\varepsilon)$ of the out-of-phase oscillations of two dark solitons grows in the limit $\varepsilon \rightarrow 0$. This property will be further discussed in section 6.

5. m -solitons with $m \geq 2$

We extrapolate the results of section 4 to the case of m -solitons with $m \geq 2$. The general superposition of m dark solitons is substituted in the form

$$v_m(x, t) = \prod_{j=1}^m (A_j(t) \tanh(\varepsilon^{-1} B_j(t)(x - a_j(t))) + i b_j(t)), \quad (22)$$

where

$$A_j = \sqrt{1 - b_j^2}, \quad B_j = \frac{1}{\sqrt{2}} \sqrt{1 - a_j^2} \sqrt{1 - b_j^2}, \quad j \in \{1, 2, \dots, m\}$$

for $a_j \in (-1, 1)$ and $b_j \in (-1, 1)$. Under the same assumptions of

$$|a_j| \leq C_1 \varepsilon^{1/6}, \quad j \in \{1, 2, \dots, m\}$$

and

$$e^{-\sqrt{2}(a_{j+1}-a_j)\varepsilon^{-1}} \leq C_2 \varepsilon^2 \log(\varepsilon), \quad j \in \{1, 2, \dots, m-1\},$$

for some $C_1, C_2 > 0$, we reduce the effective Lagrangian $L_m := L(v_m)/2\varepsilon$ to the leading order

$$L_m \sim -\sqrt{2} \sum_{j=1}^m (a_j^2 + b_j^2) - 2 \sum_{j=1}^m a_j b_j - 8\sqrt{2} \sum_{j=1}^{m-1} e^{-\sqrt{2}(a_{j+1}-a_j)\varepsilon^{-1}},$$

where only the quadratic terms in (a_j, b_j) and only the pairwise interaction potentials are taken into account. Using the Euler–Lagrange equations, we obtain

$$\dot{a}_j = \sqrt{2} b_j, \quad \dot{b}_j = -\sqrt{2} a_j - 8\varepsilon^{-1} (e^{-\sqrt{2}(a_{j+1}-a_j)\varepsilon^{-1}} - e^{-\sqrt{2}(a_j-a_{j-1})\varepsilon^{-1}}), \quad j \in \{1, 2, \dots, m\}, \quad (23)$$

where boundary conditions $a_0 = -\infty$ and $a_{m+1} = \infty$ are assumed. The centre of mass $\langle a \rangle = \frac{1}{m} \sum_{j=1}^m a_j$ satisfies the linear oscillator equation

$$\ddot{\langle a \rangle} + 2\langle a \rangle = 0, \quad (24)$$

which recovers the frequency $\sqrt{2}$ of oscillations of one dark soliton in section 3. This frequency corresponds to the in-phase oscillations of m -solitons.

Let us introduce the set of normal coordinates

$$x_j = \sqrt{2}(a_{j+1} - a_j)\varepsilon^{-1}, \quad j \in \{1, 2, \dots, m-1\},$$

and rewrite system (23) in the scalar form

$$\ddot{x}_j + 2x_j + 16\varepsilon^{-2} (e^{-x_{j+1}} - 2e^{-x_j} + e^{-x_{j-1}}) = 0, \quad j \in \{1, 2, \dots, m-1\}, \quad (25)$$

where the boundary conditions are now $x_0 = x_m = \infty$. System (25) is known as the Toda lattice with nonzero masses, which is not integrable by inverse scattering (unlike its counterpart with zero masses). We are only interested in existence of critical points in the Toda lattice and in the distribution of eigenvalues in the linearization around the critical points.

Critical points of the Toda lattice (25) are defined by solutions of the system of algebraic equations

$$2x_j + 16\varepsilon^{-2} (e^{-x_{j+1}} - 2e^{-x_j} + e^{-x_{j-1}}) = 0, \quad j \in \{1, 2, \dots, m-1\}. \quad (26)$$

Let the $(m - 1) \times (m - 1)$ matrix \mathbf{A} be given by

$$\mathbf{A} = \begin{bmatrix} 2 & -1 & 0 & 0 & \cdots & 0 & 0 \\ -1 & 2 & -1 & 0 & \cdots & 0 & 0 \\ 0 & -1 & 2 & -1 & \cdots & 0 & 0 \\ \vdots & \vdots & \vdots & \vdots & \vdots & \vdots & \vdots \\ 0 & 0 & 0 & 0 & \cdots & -1 & 2 \end{bmatrix}.$$

Matrix \mathbf{A} arises in the central-difference approximation of the second derivative subject to the Dirichlet boundary conditions. It is strictly positive and thus invertible. The system of algebraic equations (26) can be written in the matrix–vector form

$$\mathbf{A}\mathbf{e}^{-\mathbf{x}} = \frac{\varepsilon^2}{8}\mathbf{x} \Rightarrow \mathbf{e}^{-\mathbf{x}} = \frac{\varepsilon^2}{8}\mathbf{A}^{-1}\mathbf{x}. \quad (27)$$

Solutions of system (27) in the limit $\varepsilon \rightarrow 0$ are analysed in the following lemma.

Lemma 5. For sufficiently small $\varepsilon > 0$, there exists a unique solution of system (27) in the neighbourhood of ∞ , which is expanded by

$$\mathbf{x} = -2 \log(\varepsilon)\mathbf{1} - \log |\log(\varepsilon)|\mathbf{1} + 2 \log(2)\mathbf{1} - \log(\mathbf{A}^{-1}\mathbf{1}) + o(1), \quad \text{as } \varepsilon \rightarrow 0, \quad (28)$$

where $\mathbf{1} = [1, 1, \dots, 1]^T \in \mathbb{R}^{m-1}$.

Proof. Applying the natural logarithm to system (27), we rewrite the system as follows:

$$\mathbf{x} = -2 \log(\varepsilon)\mathbf{1} + 3 \log(2)\mathbf{1} - \log(\mathbf{A}^{-1}\mathbf{x}).$$

Repeating the proof of lemma 3, we find the desired expansion (28). \blacksquare

Back to the physical variables (a_1, \dots, a_m) , the result of lemma 5 implies that the coordinates of dark solitons are centred at $\langle a \rangle = 0$ and distributed with nearly equal spacing as $\varepsilon \rightarrow 0$. Linearizing the Toda lattice (25) about the root of system (26), we obtain the linear eigenvalue problem

$$(2 - \omega^2)\xi_j - 16\varepsilon^{-2} (e^{-x_{j+1}}\xi_{j+1} - 2e^{-x_j}\xi_j + e^{-x_{j-1}}\xi_{j-1}) = 0, \quad j \in \{1, 2, \dots, m-1\}, \quad (29)$$

where ξ_0 and ξ_m are not determined because the coefficients in front of ξ_0 and ξ_m are zero. Using the equivalent representation (27), we rewrite the linear eigenvalue problem in the form

$$(2 - \omega^2)\xi_j - 2((\mathbf{A}^{-1}\mathbf{x})_{j+1}\xi_{j+1} - 2(\mathbf{A}^{-1}\mathbf{x})_j\xi_j + (\mathbf{A}^{-1}\mathbf{x})_{j-1}\xi_{j-1}) = 0, \quad j \in \{1, 2, \dots, m-1\}. \quad (30)$$

Squared frequencies ω^2 of oscillations of m -solitons are analysed in the limit $\varepsilon \rightarrow 0$ in the following lemma.

Lemma 6. For sufficiently small $\varepsilon > 0$, $(m - 1)$ eigenvalues of the linear problem (30) are expanded by

$$\omega^2 = 2 + (-4 \log(\varepsilon) - 2 \log |\log(\varepsilon)| + 4 \log(2))\Omega^2 + \mathcal{O}(1), \quad (31)$$

where $\Omega^2 \in \{1, 3, 6, \dots, m(m-1)/2\}$ and $m \geq 2$.

Proof. The matrix eigenvalue problem (30) with the asymptotic expansion (28) can be written in the form

$$(2 - \omega^2)\xi_j + (4 \log(\varepsilon) + 2 \log |\log(\varepsilon)| - 4 \log(2))(v_{j+1}\xi_{j+1} - 2v_j\xi_j + v_{j-1}\xi_{j-1}) + 2(w_{j+1}\xi_{j+1} - 2w_j\xi_j + w_{j-1}\xi_{j-1}) + o(1) = 0, \quad \text{as } \varepsilon \rightarrow 0, \quad (32)$$

where $\mathbf{v} = \mathbf{A}^{-1}\mathbf{1} \in \mathbb{R}^{m-1}$ and $\mathbf{w} = \mathbf{A}^{-1} \log(\mathbf{v}) \in \mathbb{R}^{m-1}$.

Let Ω^2 be eigenvalues of the reduced eigenvalue problem

$$\Omega^2 \xi_j + v_{j+1} \xi_{j+1} - 2v_j \xi_j + v_{j-1} \xi_{j-1} = 0, \quad j \in \{1, 2, \dots, m-1\}. \quad (33)$$

We will show that all eigenvalues of the reduced eigenvalue problem (33) are simple and given explicitly by $\Omega^2 \in \{1, 3, 6, \dots, m(m-1)/2\}$. If this is the case, the regular perturbation theory for the perturbed eigenvalue problem (32) implies that

$$|\omega^2 - 2 + (4 \log(\varepsilon) + 2 \log |\log(\varepsilon)| - 4 \log(2)) \Omega^2| = \mathcal{O}(\varepsilon), \quad \text{as } \varepsilon \rightarrow 0,$$

for each eigenvalue Ω^2 .

To obtain the exact distribution of eigenvalues of the reduced eigenvalue problem (33), we will find the vector v explicitly. The components of v satisfy the Dirichlet problem for second-order difference equations

$$2v_j - v_{j+1} - v_{j-1} = 1, \quad j \in \{1, 2, \dots, m-1\},$$

subject to $v_0 = v_m = 0$. The exact solution of this problem is obtained by substitution

$$v_j = \frac{1}{2} j(m-j), \quad j \in \{1, 2, \dots, m-1\}.$$

Let $k = j - (m/2)$, so that $k \in \mathcal{I}_m := \{-(m/2) + 1, -(m/2) + 2, \dots, (m/2) - 1\}$. Note that \mathcal{I}_m includes integer values for even m and half-integer values for odd m . Denote $\zeta_k = \xi_j$ and $\lambda = 2\Omega^2$ and rewrite the reduced eigenvalue problem (33) in the following explicit form:

$$\lambda \zeta_k = \left(\frac{m^2}{4} - k^2 \right) (2\zeta_k - \zeta_{k+1} - \zeta_{k-1}) + 2k (\zeta_{k+1} - \zeta_{k-1}) + (\zeta_{k+1} + \zeta_{k-1}), \quad k \in \mathcal{I}_m. \quad (34)$$

First, we consider problem (34) for all $k \in \mathbb{Z}$ with a fixed $m \geq 2$ and prove that there exists a basis of eigenvectors $\zeta \in \{\mathcal{P}_n\}_{n \in \mathbb{N}_0}$ in the space of analytic functions on \mathbb{Z} for an infinite set of eigenvalues $\lambda \in \{(n+1)(n+2)\}_{n \in \mathbb{N}_0}$, where $\mathbb{N}_0 := \{0, 1, 2, \dots\}$. The corresponding eigenvector $\zeta = \mathcal{P}_n$ for each eigenvalue $\lambda = (n+1)(n+2)$ is given by the polynomial $\mathcal{P}_n(k)$ in the form

$$\zeta_k = \mathcal{P}_n(k) := k^n + c_1 k^{n-1} + c_2 k^{n-2} + \dots + c_n, \quad k \in \mathbb{Z}, \quad (35)$$

with uniquely determined coefficients (c_1, c_2, \dots, c_n) . To show this, we note that if $\zeta \in \mathcal{P}_n$, where \mathcal{P}_n is the vector space of polynomials of degree n , then the vector field of the eigenvalue problem (34) belongs to \mathcal{P}_n . This follows from the fact that if $\zeta \in \mathcal{P}_n$, then

$$(2\zeta_k - \zeta_{k+1} - \zeta_{k-1}) \in \mathcal{P}_{n-2}, \quad (\zeta_{k+1} - \zeta_{k-1}) \in \mathcal{P}_{n-1}, \quad (\zeta_{k+1} + \zeta_{k-1}) \in \mathcal{P}_n. \quad (36)$$

Substituting representation (35) to the linear eigenvalue problem (34), we collect coefficients in front of k^n to find that $\lambda = (n+1)(n+2)$ and the coefficients in front of $k^{n-1}, k^{n-2}, \dots, k^0$ to find a lower triangular system of linear equations for c_1, c_2, \dots, c_n . The lower triangular coefficient matrix is invertible (non-singular) because, if this is not the case, a homogeneous solution would exist to give a polynomial of a lower degree for the same eigenvalue λ . This contradicts the fact that the set $\{(n+1)(n+2)\}_{n \in \mathbb{N}_0}$ includes only simple eigenvalues. Therefore, a unique value for (c_1, c_2, \dots, c_n) exists for a given n . All eigenvectors are linearly independent since polynomials of different degrees defined on \mathbb{Z} are linearly independent. The set of all eigenvectors gives a basis of eigenvectors in the space of analytic functions on \mathbb{Z} .

Next, we will prove that the basis of eigenvectors for the linear eigenvalue problem (34) on \mathcal{I}_m with $m \geq 2$ is given by $\{\mathcal{P}_0, \mathcal{P}_1, \dots, \mathcal{P}_{m-2}\}$, which corresponds to the first $(m-1)$ eigenvalues $\lambda \in \{2, 6, 12, \dots, m(m-1)\}$. This follows from the fact that each polynomial \mathcal{P}_j is nonzero on \mathcal{I}_m for $j \in \{0, 1, \dots, m-2\}$ in the sense of

$$\sum_{k \in \mathcal{I}_m} |P_j(k)| \neq 0, \quad j \in \{0, 1, \dots, m-2\}. \quad (37)$$

Suppose for a contradiction that condition (37) is false, that is $P_j(k)$ has $(m - 1)$ roots on \mathbb{R} . However, $j < (m - 1)$ and by the fundamental theorem of algebra, $P_j(k) \equiv 0$ for all $k \in \mathbb{Z}$, which gives us the contradiction. Therefore, condition (37) is satisfied. Furthermore, since polynomials $\{P_0, P_1, \dots, P_{m-2}\}$ correspond to distinct eigenvalues, these eigenvectors are linearly independent and form a basis of eigenvectors on \mathcal{I}_m . This implies that all other polynomials in the set $\{P_j\}_{j \geq m-1}$ are linearly dependent from $\{P_0, P_1, \dots, P_{m-2}\}$ on \mathcal{I}_m , which means, in view of different degrees and distinct eigenvalues, that P_j are identically zero on \mathcal{I}_m for all $j \geq m - 1$. Therefore, the basis of eigenvectors for the linear eigenvalue problem (34) on \mathcal{I}_m with $m \geq 2$ is given by $\{P_0, P_1, \dots, P_{m-2}\}$. ■

We note that the polynomial $P_n(k)$ in (35) is even in $k \in \mathbb{Z}$ for even n and odd in $k \in \mathbb{Z}$ for odd n . This follows from the parity transformations of operators in (36) and the explicit form of the linear eigenvalue problem (34). For example, let $m = 4$ so that $\mathcal{I}_4 = \{-1, 0, 1\}$ and compute eigenvectors and eigenvalues of (34) explicitly:

$$\begin{aligned} \lambda = 2 : \quad & \zeta_k = P_0(k) = 1, \\ \lambda = 6 : \quad & \zeta_k = P_1(k) = k, \\ \lambda = 12 : \quad & \zeta_k = P_2(k) = k^2 - \frac{3}{5}. \end{aligned}$$

For the same case $m = 4$, $P_3(k) = k(k^2 - 1)$ so that $P_3(k) = 0$ for all $k \in \mathcal{I}_4$. This example illustrates the general case in the proof of lemma 6.

We finish this section with the explicit asymptotic approximations for 3-solitons ($m = 3$). By the symmetry of system (26) with $m = 3$, we understand that

$$x_1 = x_2 = \sqrt{2}a\varepsilon^{-1} \Leftrightarrow a_1 = -a, \quad a_2 = 0, \quad a_3 = a,$$

where a is a root of equation

$$a - 4\sqrt{2}\varepsilon^{-1}e^{-\sqrt{2}a\varepsilon^{-1}} = 0,$$

which is expanded asymptotically as

$$a = \frac{\varepsilon}{\sqrt{2}} (-2 \log(\varepsilon) - \log |\log(\varepsilon)| + 2 \log(2) + o(1)), \quad \text{as } \varepsilon \rightarrow 0. \quad (38)$$

Comparison with the asymptotic expansion (28) shows that $v = \mathbf{1}$ and $w = A^{-1} \log(v) = \mathbf{0}$. Therefore, the perturbed eigenvalue problem (32) for $m = 3$ has no $\mathcal{O}(1)$ term related to w and the asymptotic distribution (31) becomes accurate with $\mathcal{O}(1)$ replaced by $o(1)$. As a result, we find the explicit asymptotic expansions of the two squared frequencies of the out-of-phase oscillations of 3-solitons:

$$\begin{cases} \omega^2 = 2 + (-4 \log(\varepsilon) - 2 \log |\log(\varepsilon)| + 4 \log(2)) + o(1), \\ \omega^2 = 2 + 3(-4 \log(\varepsilon) - 2 \log |\log(\varepsilon)| + 4 \log(2)) + o(1). \end{cases} \quad (39)$$

These asymptotic results will be tested numerically in section 6.

6. Numerical results

We now compare the asymptotic results with direct numerical results for the existence and spectral stability of 2- and 3-soliton configurations. We identify the relevant branches of stationary solutions by solving the ordinary differential equation

$$-\frac{1}{2}v''(\xi) + \frac{1}{2}\xi^2 v(\xi) + v^3(\xi) - \mu v(\xi) = 0, \quad \xi \in \mathbb{R}. \quad (40)$$

A fixed point method (Newton–Raphson iteration) is used to solve a discretized boundary-value problem, after a centred-difference scheme is applied to the second-order derivatives

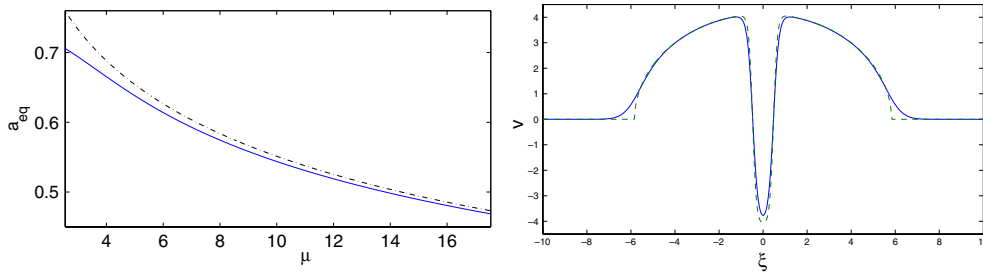


Figure 1. Left: the equilibrium position of the two dark solitons versus the chemical potential μ . The solid line shows the direct numerical result and the dashed–dotted line represents the asymptotic approximation (18). Right: the solid line shows the numerical solution $v(\xi)$ for $\mu = 17$, while the dashed line represents the corresponding variational ansatz.

with a typical spacing of $\Delta\xi = 0.025$. The resulting solutions $v(\xi)$ are obtained starting from the corresponding linear eigenfunction (with 2- or 3-nodes at the linear limit) and continuation over the values of the chemical potential parameter μ is used in order to extend the branch to the large values of μ . Similar numerical techniques were used in [12, 22]. Note that the existence and spectral stability of the 1-soliton configuration were examined in our earlier work in [15].

Once the stationary solution is obtained for each value of μ , we linearize around it, using an ansatz of the form

$$v(\xi, \tau) = v(\xi) + \delta \left(a(\xi)e^{\lambda\tau} + \bar{b}(\xi)e^{\bar{\lambda}\tau} \right), \quad (41)$$

where δ denotes a formal (small) parameter. The admissible values of λ (eigenvalues) are found from the condition that $(a, b) \in L^2(\mathbb{R})$ is a solution of the linear eigenvalue problem

$$\begin{cases} -\frac{1}{2}a''(\xi) + \frac{1}{2}\xi^2a(\xi) - \mu a(\xi) + v^2(\xi)(2a(\xi) + b(\xi)) = i\lambda a(\xi), \\ -\frac{1}{2}b''(\xi) + \frac{1}{2}\xi^2b(\xi) - \mu b(\xi) + v^2(\xi)(a(\xi) + 2b(\xi)) = -i\lambda b(\xi). \end{cases} \quad (42)$$

Using again a discretization of the differential operators on the same grid, we reduce (42) to a matrix eigenvalue problem which can be solved through standard numerical linear algebra routines.

Our main results are summarized in figures 1 and 2 for the 2-soliton configuration and figures 3 and 4 for the 3-soliton case.

Figure 1 compares the numerical result (solid line) for the location of zeros of $v(\xi)$ with the asymptotic expansion (18) (dashed–dotted line), where the scaling transformation (2) has been taken into account to translate the results from ε to μ by $\varepsilon = (2\mu)^{-1}$. One can see that the asymptotic expansion yields a highly accurate approximation of the numerical result. This is also evidenced by the right panel of the figure comparing the numerical solution $v(\xi)$ for $\mu = 17$ (solid line) with the variational ansatz (dashed line).

Figure 2 shows the smallest eigenvalues of the linear eigenvalue problem (42) obtained numerically (solid line). The resulting eigenvalues can be classified into two groups. The first one consists of a countable set of pairs of purely imaginary eigenvalues that give frequencies of oscillations of the ground state. The frequencies of oscillations of the ground state η_ε are found in the limit $\varepsilon \rightarrow 0$ as follows [7]:

$$\lim_{\varepsilon \rightarrow 0} \omega_n(\varepsilon) = \sqrt{2n(n+1)}, \quad n \geq 1.$$

Note that $\omega_1(\varepsilon) = 2$ is preserved for any $\varepsilon > 0$ thanks to the symmetry of the Gross–Pitaevskii equation with a harmonic potential [15]. Using the scaling transformation (2), we conclude

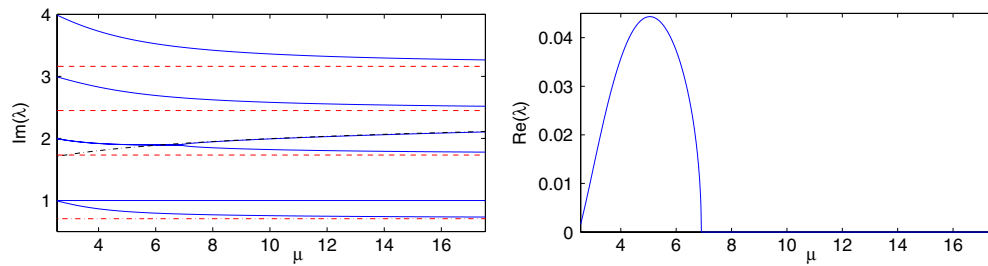


Figure 2. Left: solid lines indicate the frequencies of linearization around a 2-soliton solution as a function of the chemical potential μ . The dashed lines show the asymptotic limits (43) for the frequencies around the ground state. The dashed–dotted lines indicate the asymptotic predictions for the in-phase (lower frequency) and out-of-phase (higher frequency) oscillations of 2 dark solitons. Right: real part of the unstable eigenvalue in a finite instability band near the linear limit.

that these frequencies satisfy the asymptotic limit

$$\lim_{\mu \rightarrow \infty} \text{Im}(\lambda) = \frac{\sqrt{n(n+1)}}{\sqrt{2}}, \quad n \geq 1. \quad (43)$$

The asymptotic limits (43) are shown in figure 2 by dashed lines.

The second group of eigenvalues consists of only two pairs of eigenvalues and is associated with the relative motions of the dark solitons [20]. One pair of eigenvalues corresponds to the in-phase oscillations with frequencies $\text{Im}(\lambda) \sim \frac{1}{\sqrt{2}}$ as $\mu \rightarrow \infty$ (or $\omega \sim \sqrt{2}$ as $\varepsilon \rightarrow 0$ in notations of the linear oscillator equation (24)). The other pair of eigenvalues corresponds to out-of-phase oscillations and it is characterized by the asymptotic expansion (21). The asymptotic predictions for these frequencies are shown by the dashed–dotted lines.

The right panel of figure 2 shows the real part of the eigenvalues close to the limit of local bifurcation at $\mu = \frac{5}{2}$. The instability, which was studied in [22], is caused by the resonance between the out-of-phase 2-soliton oscillations and the quadrupolar oscillation mode of the ground state. However, the instability interval is finite and the 2-soliton excited state is linearly stable for sufficiently large values of the chemical potential μ (only small values of μ were considered in [22]).

We note, however, that the frequency $\omega_0(\varepsilon)$ of the out-of-phase oscillations of two dark solitons given by the asymptotic expansion (21) grows as $\varepsilon \rightarrow 0$. As a result, this frequency will coalesce with other frequencies $\omega_n(\varepsilon)$, $n \geq 3$ associated with oscillations of the ground state as $\varepsilon \rightarrow 0$. Coalescence with the frequency $\omega_3(\varepsilon)$ does not produce an instability, because of the different parity of the corresponding eigenfunctions. However, coalescence with the frequency $\omega_4(\varepsilon)$ will produce the instability again and it will happen roughly at $\varepsilon \sim e^{-10}$. This value of ε is too small to be confirmed by our numerical results in figure 2. This secondary instability of the 2-soliton excited state is anticipated in a tiny interval near $\varepsilon \sim e^{-10}$, after which the neutrally stable frequency $\omega_0(\varepsilon)$ will reappear until further such coalescence occurrences arise with frequencies $\omega_6(\varepsilon)$, $\omega_8(\varepsilon)$, etc.

Figures 3 and 4 illustrate similar characteristics but for the 3-soliton state. Once again the variational prediction given by the asymptotic expansion (38) provides a highly accurate estimate of the numerical inter-soliton distance $a = a_3 - a_2 = a_2 - a_1$.

On the other hand, in this case, there exist three frequencies associated with the relative motions of three dark solitons, whose values can be seen to be in very good agreement with the asymptotic expansion (39). Close to the linear limit $\mu = \frac{7}{2}$, there exist two resonances between out-of-phase motion of three dark solitons and the corresponding frequencies of oscillations

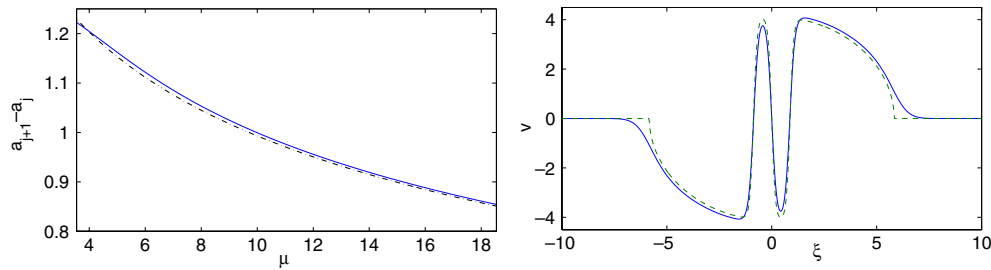


Figure 3. Similar to figure 1 but for the 3-soliton case. The left panel again shows the equilibrium inter-soliton distance (solid: numerical results; dashed–dotted: asymptotic approximation), while the right panel shows the numerical prediction (solid) and variational ansatz (dashed) of the 3-soliton state $v(\xi)$ for $\mu = 17$.

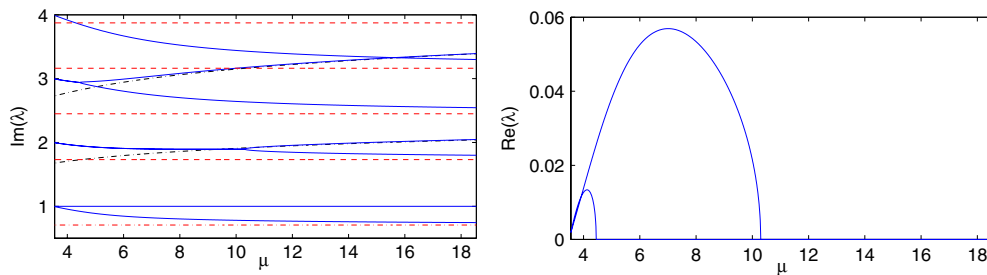


Figure 4. Same as figure 2, but for the 3-soliton case. The left panel shows the numerical frequencies (imaginary parts of the relevant eigenvalues) by solid line, the asymptotic limits for the frequencies of the ground state by dashed line and the frequencies of oscillations of three dark solitons by dashed–dotted line. The right panel illustrates the real part of the unstable eigenmodes arising close to the linear limit.

of the ground state. The two resonances induce instabilities of the 3-soliton excited states with two finite instability bands.

A general summary of the bifurcations observed in this system could be given as follows: the bound state of m dark solitons possesses m frequencies associated with the ‘normal modes’ of the m th excited state. Of these, the lowest one always corresponds to the in-phase oscillations of the dark solitons and is always below the unit frequency associated with the μ -independent oscillation of the ground state. Hence, this frequency does not lead to any resonances or collisions with other frequencies. However, *generically* all remaining $m - 1$ frequencies associated with the m th excited state lead to resonances with other frequencies in the vicinity of the linear limit. These resonances will cease to exist at some critical μ ; however, for larger values of μ , further such resonances arise, because the frequencies grow logarithmically with larger values of μ .

The above results provide a relatively complete understanding of the statics and near-equilibrium dynamics of multi-soliton states within BECs at least within the large density limit. This characterization is especially relevant presently given the recent experiments of [20, 21] enabling the observation and robust time-following for large timescales (of the order of hundred milliseconds or more) of such states. However, there would be a multitude of directions in which it would be relevant to generalize these results, if possible. On the one hand, extending them (analytically) to non-polynomial variants of the Gross–Pitaevskii equation accounting for the confinement of the condensate across transverse directions would be a challenging theoretical task. Another equally interesting direction would involve attempting to generalize

relevant notions in trying to characterize the dynamics of vortex solitons in higher dimensional settings. These directions are presently under consideration and new results will be reported in future publications.

Acknowledgments

MC is supported by the NSERC USRA scholarship, DEP is partially supported by the NSERC grant and PGK is partially supported by NSF-DMS-0349023 (CAREER), NSF-DMS-0806762 and the Alexander-von-Humboldt Foundation.

References

- [1] D'Agosta R, Malomed B A and Presilla C 2002 Stationary states of Bose–Einstein condensates in single- and multi-well trapping potentials *Laser Phys.* **12** 37–42
- [2] D'Agosta R and Presilla C 2002 States without a linear counterpart in Bose–Einstein condensates *Phys. Rev. A* **65** 043609
- [3] Alfimov G L and Zezyulin D A 2007 Nonlinear modes for the Gross–Pitaevskii equation—a demonstrative computation approach *Nonlinearity* **20** 2075–92
- [4] Anderson B P, Haljan P C, Regal C A, Feder D L, Collins L A, Clark C W and Cornell E A 2001 Watching dark solitons decay into vortex rings in a Bose–Einstein condensate *Phys. Rev. Lett.* **86** 2926–9
- [5] Burger S, Bongs K, Dettmer S, Ertmer W, Sengstock K, Sanpera A, Shlyapnikov G V and Lewenstein M 1999 Dark solitons in Bose–Einstein condensates *Phys. Rev. Lett.* **83** 5198–201
- [6] Carretero-González R, Frantzeskakis D J and Kevrekidis P G 2008 Nonlinear waves in Bose–Einstein condensates: physical relevance and mathematical techniques *Nonlinearity* **21** R139–202
- [7] Gallo C and Pelinovsky D 2009 Eigenvalues of a nonlinear ground state in the Thomas–Fermi approximation *J. Math. Anal. Appl.* **355** 495–526
- [8] Gallo C and Pelinovsky D 2009 On the Thomas–Fermi ground state in a radially symmetric parabolic trap [arXiv:0911.3913](https://arxiv.org/abs/0911.3913)
- [9] Engels P and Atherton C 2007 Stationary and nonstationary fluid flow of a Bose–Einstein condensate through a penetrable barrier *Phys. Rev. Lett.* **99** 160405
- [10] Ignat R and Millot V 2006 The critical velocity for vortex existence in a two-dimensional rotating Bose–Einstein condensate *J. Funct. Anal.* **233** 260–306
- [11] Ignat R and Millot V 2006 Energy expansion and vortex location for a two-dimensional rotating Bose–Einstein condensate *Rev. Math. Phys.* **18** 119–62
- [12] Kivshar Y S, Alexander T J and Turitsyn S K 2001 Nonlinear modes of a macroscopic quantum oscillator *Phys. Lett. A* **278** 225–30
- [13] Konotop V V and Pitaevskii L 2004 Landau dynamics of a grey soliton in a trapped condensate *Phys. Rev. Lett.* **93** 240403
- [14] Kivshar Yu S and Krolikowski W 1995 Lagrangian approach for dark solitons *Opt. Commun.* **114** 353–62
- [15] Pelinovsky D E and Kevrekidis P G 2008 Periodic oscillations of dark solitons in parabolic potentials *AMS Contemp. Math.* **473** 159–80
- [16] Pethick C J and Smith H 2002 *Bose–Einstein Condensation in Dilute Gases* (Cambridge: Cambridge University Press)
- [17] Pitaevskii L and Stringari S 2003 *Bose–Einstein Condensation* (Oxford: Oxford University Press)
- [18] Shomroni I, Lahoud E, Levy S and Steinhauer J 2009 Evidence for an oscillating soliton/vortex ring by density engineering of a Bose–Einstein condensate *Nature Phys.* **5** 193–7
- [19] Stellmer S, Becker C, Soltan-Panahi P, Richter E-M, Dörscher S, Baumert M, Kronjäger J, Bongs K and Sengstock K 2008 Collisions of dark solitons in elongated Bose–Einstein condensates *Phys. Rev. Lett.* **101** 120406
- [20] Theocharis G, Weller A, Ronzheimer J P, Gross C, Oberthaler M K, Kevrekidis P G and Frantzeskakis D J 2010 Multiple atomic dark solitons in cigar-shaped Bose–Einstein condensates *Phys. Rev. A* **81** 063604
- [21] Weller A, Ronzheimer J P, Gross C, Esteve J, Oberthaler M K, Frantzeskakis D J, Theocharis G and Kevrekidis P G 2008 Experimental observation of oscillating and interacting matter wave dark solitons *Phys. Rev. Lett.* **101** 130401
- [22] Zezyulin D A, Alfimov G L, Konotop V V and Pérez-García V M 2008 Stability of excited states of a Bose–Einstein condensate in an anharmonic trap *Phys. Rev. A* **78** 013606